Neuroscience and Biobehavioral Reviews 169 (2025) 105988

Contents lists available at ScienceDirect

Neuroscience and Biobehavioral Reviews

journal homepage: www.elsevier.com/locate/neubiorev

Turbulence as a framework for brain dynamics in health and disease

Gustavo Deco [a,b,*], Yonatan Sanz Perl [a,c], Katarina Jerotic [d,e,f], Anira Escrichs [a], Morten L. Kringelbach [d,e,f,**]

[a] Center for Brain and Cognition, Computational Neuroscience Group, Department of Information and Communication Technologies, Universitat Pompeu Fabra, Roc Boronat 138, Barcelona 08018, Spain
[b] Institució Catalana de la Recerca i Estudis Avançats (ICREA), Passeig Lluís Companys 23, Barcelona 08010, Spain
[c] Department of Physics, University of Buenos Aires, Buenos Aires, Argentina
[d] Centre for Eudaimonia and Human Flourishing, Linacre College, University of Oxford, Oxford, UK
[e] Department of Psychiatry, University of Oxford, Oxford, UK
[f] Center for Music in the Brain, Department of Clinical Medicine, Aarhus University, Aarhus, Denmark

ARTICLE INFO

Keywords:
Turbulence
Coupled oscillators
Scale-free
Brain dynamics

ABSTRACT

Turbulence is a universal principle for fast energy and information transfer. Moving beyond the turbulence of fluid dynamics, turbulence has recently been demonstrated in brain dynamics. Importantly, turbulence can be expressed as the rich variability across spacetime of the local levels of synchronisation of coupled brain signals. In fact, the optimal mixing properties of turbulence is what allows for efficient transfer of energy/information over space and time in the brain. This is especially important for survival given the need to overcome the inherent slowness in neural dynamics. Here, we review the research showing that the turbulence offers a convenient framework for describing brain dynamics and that the scale-free nature of turbulence, reflected in power-laws, provides the necessary mechanisms for time-critical information transfer in the brain. Whole-brain modelling of turbulence as coupled-oscillators has been shown to provide precise signatures of many different brain states. The levels of turbulence change in disease, and careful research of the vortex space could potentially help discover new avenues for a better understanding of this breakdown and offer better control of these highly non-linear, non-equilibrium states. Overall, the framework of the turbulent brain is a highly fertile, fast developing field with great potential.

1. Introduction

"Big whirls have little whirls / That feed on their velocity, / And little whirls have lesser whirls / And so on to viscosity …".

Lewis Fry Richardson (1881–1953)

"Let no-one who is not a mathematician read my principles".

Leonardo da Vinci (1452–1519)

A major question in our pursuit of understanding the mind is the paradox of how quickly the brain is able to respond and adapt to change despite the underlying slowness of neuronal processes. Indeed, rates of information transfer between neurons are surprisingly slow, on the order of approximately 10–20 ms (Itoh et al., 2022) as shown by the Nobel prizewinning research of Hodgkin and Huxley (Hodgkin and Huxley, 1952b). This slowness is rooted in the fact that electrical signals in the myelinated fibres must be converted to a chemical signal at the synaptic junction before being converted back to an electrical signal (Cotterill, 2002). The speed of information transfer is several orders of magnitude slower than that found in silicon-based computers, yet the brain is clearly better at solving hard problems with often minimal information and using much smaller amounts of energy. This problem of how the brain overcomes the limitations of speed for information transfer across spacetime has been a longstanding conundrum in the field of neuroscience. In this perspective, we show that part of the answer comes from the principles of turbulence in non-reversible

* Corresponding author at: Center for Brain and Cognition, Computational Neuroscience Group, Department of Information and Communication Technologies, Universitat Pompeu Fabra, Roc Boronat 138, Barcelona 08018, Spain.
** Corresponding author at: Centre for Eudaimonia and Human Flourishing, Linacre College, University of Oxford, Oxford, UK.
E-mail addresses: gustavo.deco@upf.edu (G. Deco), morten.kringelbach@psych.ox.ac.uk (M.L. Kringelbach).

https://doi.org/10.1016/j.neubiorev.2024.105988
Received 25 August 2024; Received in revised form 8 December 2024; Accepted 19 December 2024
Available online 22 December 2024

dynamical regimes taking place far from thermodynamic equilibrium, showing strong temporal asymmetry and obeying so-called power laws, providing scale-freeness (see Glossary) as the basis of efficient information transfer. This significant increase in speed from scale-free information transfer is over and above any increases in speed from parallel processing. In fact, here we show how turbulence, as a form of deterministic spatiotemporal chaos (Frisch, 1995), provides a convenient framework which can be understood as a mechanistic operationalisation of spacetime brain dynamics within a promising new field of neuroscience which we have previously termed "thermodynamics of mind" (Kringelbach et al., 2024). This new theory describes brain dynamics in terms of non-equilibrium thermodynamics and production entropy, and thus establishing a link with turbulence, which recently received confirmation by the findings of Yao and colleagues in field of fluid dynamics (Yao et al., 2024).

In order to survive in a complex world, the brain has to mix a large amount of information across space and time. This mixing is exactly what turbulence has been shown to facilitate. Originally coined as "turbolenza" (from the Latin word for 'crowdiness' or disturbed) by Leonardo DaVinci over half a millennium ago (Deco et al., 2021a) and subsequently developed by many mathematicians, turbulence is ubiquitous in Nature as an essential dynamical regime facilitating efficient energy and information transfer across spatiotemporal scales (Cross and Hohenberg, 1993).

In fact, recently, we discovered turbulence in empirical whole-brain dynamics (Deco and Kringelbach, 2020). Rather than focusing on just the signal as with most methods, we characterised the local level of synchronisation across space and time (roughly comparable to vortices in fluid dynamics). Intuitively, any system that has high variability of this local level of synchronisation is turbulent and with this comes all the important properties needed for information transfer. More formally, the Russian mathematician Andrey Kolmogorov demonstrated the efficiency of turbulence by finding a spatial power scaling law in fluid dynamics, revealing a cascade of energy and information in fluids (Kolmogorov, 1941a, b) (see excellent review in (Frisch, 1995)). This provides the basis for highly efficient energy transmission.

Beyond the limited domain of fluid dynamics, the physicist Yoshiki Kuramoto was able to generalise turbulence to other physical systems including coupled oscillators (Kuramoto, 1984), which has been shown to be an excellent basis for describing brain dynamics (Deco et al., 2017b; Kringelbach and Deco, 2020). This is important, since mathematical research has more generally shown that information transfer is analogous to energy transfer, as demonstrated by the close links between vortex propagation of disturbances and the transmission of information (Cross and Hohenberg, 1993; Oono and Yeung, 1987). Within the context of turbulence in the brain, information transfer can therefore be formally defined as the hierarchical transfer of information across scales (for a mathematical definition, see Eq. 13 in the Appendix). In fact, the rotational, spiral-like vortices in fluid dynamics can also be found in brain dynamics where oscillatory vortices spin around their phase singularity centres (Xu et al., 2023). As such, vortices can be described using the local Kuramoto parameter characterising the local level of synchronisation of their phases (see Eqs. 4 and 7 in the Appendix). These oscillating brain vortices are very similar to those found in the turbulence of other complex physical and biological systems (Bewley et al., 2006; Christoph et al., 2018).

In this perspective, we show the important implications and findings arising discovering turbulence in the local metastability of brain dynamics and modelling the brain with turbulent coupled oscillators. This complements other attempts to formulate a general theory of brain function such as the free energy principle (Friston, 2010) but crucially focusing on spacetime mechanisms of information transfer in brain function. Other important spacetime theories of consciousness include Global Workspace (Baars, 1989; Deco et al., 2021c; Dehaene et al., 1998), Integrated Information Theory (Tononi et al., 1994) and the Temporo-spatial Theory of Consciousness (Northoff, 2013, 2024; Northoff and Huang, 2017). Here, we first describe how, moving beyond just correlational measures, it is straightforward to create a whole-brain modelling framework of turbulence given that brain dynamics can be described by a whole-brain model of coupled oscillators and in particular the *Hopf whole-brain model* (Deco et al., 2017b), describing the behaviour of a Stuart-Landau non-linear oscillating system (Hopf, 1942). Second, the level of turbulence has been shown to distinguish different empirical brain states including different forms of coma, sleep (Escrichs et al., 2022) and psychedelics (Cruzat et al., 2022). Third, brain dynamics also exhibit a turbulent power law similar to that found for fluid dynamics, strongly suggesting the presence of a cascade of efficient information processing across scales needed for fast whole-brain distributed processing (Deco and Kringelbach, 2020). Finally, pointing towards the relevance of turbulence for higher order brain function, evidence has been found of higher order structure-functions demonstrating multi fractality and turbulence (Perl et al., 2023a).

2. A brief history of turbulence

Leonardo DaVinci constantly explored the capacity of pre-Newtonian laws of dynamics to lead to the complexity observed in nature (for his most developed discussions of water, see the *Codex Leicester* (Laurenza and Kemp, 2019)). Achieving an accurate drawing of the complexity of turbulent motion was extremely difficult, not least when he tried to draw the incessant movements of intersecting bodies of water, especially since it was not possible for him to freeze movement in time. Instead, he needed to develop a deep understanding of the underlying ordered mechanisms creating disorder. In fact, he was forced to use mathematics to explain the complexity of fluids in motion in a pioneering way.

With his powers of observation, Leonardo was fully aware of the ordered layered fashion of flow of water in a river, now termed *laminar flow*. He studied how a sudden obstacle like a branch in a river can create turbulent flow, resulting in varying types of vortices or eddies. Laminar flow is beautiful but ultimately rather boring from a dynamics point of view, while turbulent flow is seemingly chaotic but incredibly useful. For example, when cooking, laminar flow (stirring the spoon in repetitive, predictable circular movements) does not allow for proper mixing of the ingredients, but when you introduce more complex stirring patterns, and thus turbulence, much more efficient mixing occurs.

Merging art and science seamlessly, Leonardo discerned and represented underlying orders in what appeared to be disordered natural phenomena. His detailed analyses of the behaviour of water combine mathematical theories of motion, as understood at the time, with acute observation. His quest to embrace complexity is reflected in how he used Italian vernacular to describe his observations. At one point he listed 68 terms that might describe the varieties of fluid motion and their many effects, eventually decided on using 'turbolenza' to encompass them all.

Leonardo's characterisation of eddies at varied scales remarkably predates the seminal observations by the English polymath Lewis Fry Richardson (1881–1953), pioneer of the mathematical weather forecasting, who described the important turbulent *energy cascade principle*. As shown by Leonardo, fluids have differently sized vortices or eddies, where each corresponds to a rotational movement. The interactions between larger and smaller eddies interchange energy, in the form of velocity or kinetic energy; this is called the energy cascade and transfers energy across scales, which roughly correspond to the size of different eddies.

This energy cascade was described in a humorous verse above by Richardson, as a play on words from *Siphonaptera*, the taxonomic order of fleas, a brief poem by Augustus De Morgan, rewording Jonathan Swift: "*Great fleas have little fleas upon their backs to bite 'em; And little fleas have lesser fleas, and so ad infinitum*".

Also focusing on fluid dynamics, Kolmogorov published his groundbreaking phenomenological theory of turbulence over 80 years ago (Kolmogorov, 1941a, b). This highly influential theory demonstrates a

fundamental power scaling law, revealing the key underlying mechanisms of fluid dynamics, namely the energy cascades that balance kinetics and viscous dissipation (Fig. 1**A**). This spatial power-scaling law is a hallmark of turbulence and provides a mathematical description of Richardson's earlier concept of cascaded eddies (Richardson, 1922).

Kolmogorov's approach successfully overcomes the severe limitations of the prevailing description of turbulence at the time, which described the movement of each particle of the fluid mathematically. These fundamental movements are described by the Navier-Stokes equations, named after the French engineer Claude-Louis Navier and the British mathematician George Gabriel Stokes (Navier, 1823; Stokes, 1843). The idea was to apply these equations to microscopic elements of the fluid to infer or construct the macroscopic laws governing the whole fluid. Such an approach to the study of fluid dynamics at the microscopic level resulted in comparably little success given the large computational power needed, but unavailable at the time.

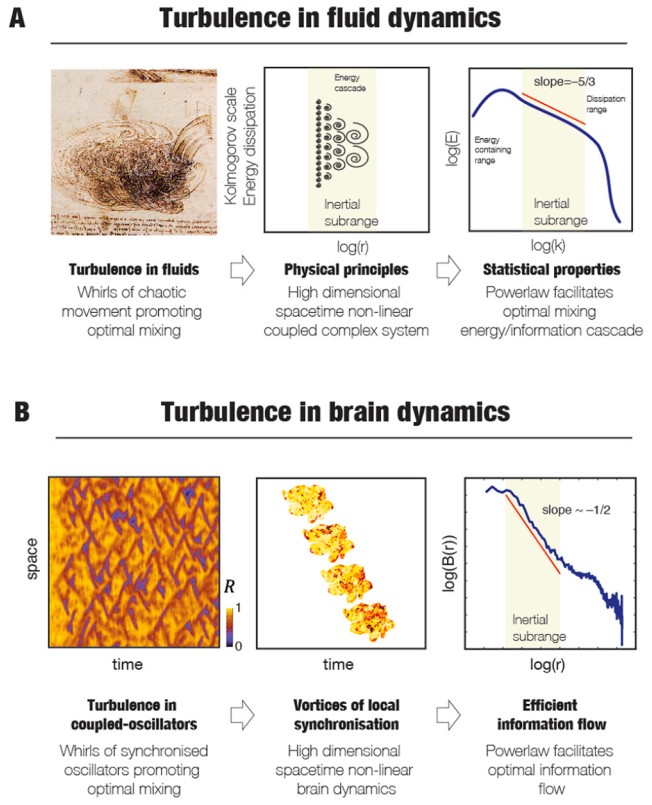

Fig. 1. Power laws for measuring turbulence in fluid dynamics and brain activity. A) The study of turbulence started with the study of fluids. Leonardo da Vinci coined "turbolenza" to describe the whirls of chaotic movement which promotes optimal mixing. Over the following centuries, the underlying physical principles were worked out, culminating in Kolmogorov's phenomenological theory of turbulence which is based on the concept of structure functions, inspired by Richardson's concept of cascading eddies. This allowed him to describe the statistical properties of the high dimensional space non-linear fluid dynamics. By doing this, Kolmogorov discovered the power laws in an inertial subrange where the structure functions show a universal energy scaling of $k^{-5/3}$, where k is the associated wave number of the spectral scale. This power law behaviour reflects the energy/information transfer cascade found in turbulence. **B)** More recently, Kuramoto was able to show turbulence in non-fluid dynamics. He used coupled-oscillators to describe the turbulent whirls of synchronised oscillators promoting optimal mixing. Specifically, he defined a local order parameter which represents a spatial average of the complex phase factor of the local oscillators weighted by the coupling. The standard deviation of the modulus of this measure defines the level of amplitude turbulence, which is shown in the left panel for a ring of Stuart-Landau oscillator system (Kawamura et al., 2007). Whole-brain neuroimaging offers the potential to obtain precise measurements of activity. The phases of these timeseries can be described over time and space by the local Kuramoto order parameter, which in turn reflects the amplitude turbulence rendered at different time steps on a flattened hemisphere of the brain. This captures the evolution of the rich variability of the whirls of local synchronisation in brain dynamics. In turn, this has been shown to follow a power law in the inertial subrange for the correlation B(r) as a function of r. This reflects the optimality of efficiency of spacetime information flow in brain dynamics.

There are strong parallels to the way that the scientists have tried — and failed — to describe the macroscopic behaviour of the brain by modelling each microscopic neuron with the Hodgkin–Huxley equations (Hodgkin and Huxley, 1952a). These were named after the Nobel prizewinning British physiologists Alan Hodgkin and Andrew Huxley, who described the activity of neurons by modelling the ionic mechanisms underlying the initiation and propagation of activity in the squid giant axon.

There are severe computational limitations with the idea of reconstructing macroscopic properties from microscopic descriptions such as the Navier-Stokes equation for fluid dynamics and Hodgkin-Huxley equations for neural dynamics. Instead, the study of turbulence is better described by the statistical approach started by Kolmogorov's vital insight. On an abstract level, Kolmogorov's approach is a way to discover order in disorder, which is, of course, exactly the same approach used by Leonardo over 500 years ago when he tried to characterise the ordered vortex configurations of crowded, disordered turbulent flows in fluids. Similar to the case of fluids, it is clear that brain activity should be described statistically directly at the macroscopic level.

As it happens, a more general form of coupled oscillators, namely non-linear oscillators can also generate turbulence. Building on previous important work starting in the 1940s, Kuramoto was able to show in the 1980s that coupled oscillators can describe turbulence in many different physical system (Kuramoto, 1984).

3. Turbulent power laws in fluid and brain dynamics

Specifically, Kolmogorov's phenomenological theory of turbulence introduced the important concept of *structure functions*, which are based on computing the spatial correlations between any two points in a fluid. He was able to demonstrate a fundamental power scaling law revealing the underlying key mechanisms of fluid dynamics, namely the energy cascades that balance kinetics and viscous dissipation. This spatial power scaling law is a hallmark of turbulence and appears at an intermediate spatial range called the "inertial subrange" where kinetic energy is not dissipated, and merely transferred to smaller scales following Richardson's concept of *cascaded eddies* (Richardson, 1922) (Fig. 1**A**, middle panel). In that inertial subrange, what Kolmogorov called '*structure functions*' (usually denoted $S(r)$) show a universal scaling factor of $r^{2/3}$ and an energy scaling of $k^{-5/3}$, where r is the spatial scale and k the associated wave number of the spectral scale (see Fig. 1**A**, right panel). Crucially, Kolmogorov demonstrated that at small scales turbulence is homogeneous isotropic and universal. In other words, the existence of power laws means that turbulence is a scale-free phenomenon. In particular, his approach was very successful in overcoming the severe limitations of inferring macroscopic laws from microscopic principles.

We hypothesised that Kolmogorov's approach using 'structure functions' would also be useful for neuroscience, especially given that the brain dynamics ultimately come from the spiking behaviour of neurons described by the Hodgkin-Huxley equations, which are a similar set of microscopic differential equations to the Navier-Stokes. Similarly to fluid dynamics, using Hodgkin-Huxley equations is inappropriate for explaining whole-brain brain dynamics (Fregnac, 2017) similar to the situation in turbulence research before Kolmogorov's vital insight.

Kolmogorov's 'structure functions' should not be confused with the structure function relations in neuroimaging. But they are highly useful and can be used to uncover the fundamental principles of brain

dynamics at the macroscopic level using large Human Connectome Project (HCP) database with resting state data from 1003 healthy human participants. To discover if human brain dynamics are organised around a *homogeneous isotropic functional core*, we used the 'structure functions' on the spatiotemporal fMRI BOLD signals from the HCP resting state data (applying the Schaefer parcellation of 1000 parcels). This empirical analysis allowed us to find a *homogeneous isotropic functional core* and *turbulent-like power scaling law* for the average functional correlations in a broad spatial range.

We explored whether power laws exist in the inertial subrange sustaining the functional core for both $S(r)$ and found that both fulfil a power law (Deco and Kringelbach, 2020). The findings clearly show this for the inertial subrange, similar to Kolmogorov's observations in fluid dynamics. The results show a power scaling law for $S(r)$ with an exponent of approximately 1/2 in the range between $r = 8.13$ mm and $r = 33.82$ mm in the inertial subrange coinciding with the functional core. Equally, the functional correlation between two nodes, $B(r)$, is computed as a function of the distance between those nodes (averaged across nodes and time), that is using homogenous isotropy (see Fig. 1**B**, right panel). Again, this obeys a power law, here with a negative exponent of approximately $-1/2$ in the same inertial subrange in the functional core.

Interestingly, in their pioneering research on wave turbulence and energy cascade in the local field potentials found in the mice hippocampus, Maurer and colleagues observed a striking similarity between the standard turbulence model and LFP spectral evolution (Sheremet et al., 2019). This observation led to their speculation that power in the theta band is the source of energy at microscopic level, while higher frequencies correspond to the inertial subrange, allowing for a cross-scale energy flow. Importantly, they also speculated that the observed peak in the gamma band is similar to the bottleneck effect in hydrodynamics and can thus be interpreted as the existence of a transitional scale right above microscopic with a limited energy-flux ability.

Beyond this initial power law, we note that a defining property in turbulence systems is that they deviate from perfect scale invariance. Many critical systems are scale invariant, such as, for example, critical phase transitions (Cocchi et al., 2017). Turbulence is an out-of-equilibrium forced and dissipative system which has deviations from scale invariance characterising how perturbations are transported and dissipated. One scaling law (or, equivalently, one critical exponent) is unable to capture turbulent deviations from equilibrium, and higher order critical exponents are needed to identify this behaviour.

This led to the question of whether the different scaling laws in turbulent fluid dynamics are also found in turbulent neuronal dynamics. Sanz Perl and colleagues used this equation on HCP neuroimaging data from over 1000 participants to discover a spatial power law scaling of higher-order structure functions $S_p(r)$ as a function of $\log(r)$ within the inertial subrange (Perl et al., 2023a). These results suggest that human brain dynamics display at least a bi-fractal structure. This turbulent behaviour is reminiscent of the case of fluids following the Burgers equation, where the departure from mono-fractality and saturation of the scaling exponents is associated with large-scale intermittency in a disordered system (Bouchaud et al., 1995). This observation is also aligned with findings of multifractality in brain dynamics, and important principles of fractality are revealed in a number of key articles (Kelty-Stephen et al., 2013; Likens et al., 2015). Overall, this shows that human brain dynamics are clearly turbulent, allowing for efficient information transfer across spacetime.

4. Turbulence generated by coupled oscillators

Moving beyond general power laws, it is important to get closer to the local dynamics of turbulence. Important for this approach is the seminal finding by Kuramoto (shown in Fig. 1**B**, left panel), namely that coupled oscillators exhibiting local synchronisations give rise to turbulence in a non-fluid context (Kuramoto, 1984). This uses the concept of 'local metastability', which is measuring the local level of synchronisation of the coupled oscillators and thereby capturing brain signal variation across spacetime. In general, metastability is a very useful concept from the dynamical systems literature which can be used to capture the balance between integration and segregation needed for healthy brain dynamics (Hancock et al., 2024; Kelso, 1995). But metastability can be found in many systems as demonstrated by Kelso and colleagues who developed a mathematical model to explain the metastable behaviour observed in bimanual coordination studies of finger flexing with a pacing metronome (Kelso, 1995).

In the context of brain dynamics, turbulence can be measured as the local metastability, defined by local synchronisation levels at varying spatial scales, λ, by means of the local Kuramoto order parameter R_λ, therefore providing a measure of local vorticity. In other words, turbulence is defined as the spacetime variability of the local metastability measured by the local Kuramoto order parameter, which is in essence an extension of the concept of global metastability (Kawamura et al., 2007) (Eq. 4 in Appendix). The global metastability has been applied in neuroscience as the global Kuramoto order parameter – a measure of temporal variability of the *global* synchronisation level of the whole system (Cabral et al., 2014; Kitzbichler et al., 2009; Kuramoto, 1984; Shanahan, 2010; Tognoli and Kelso, 2014; Wildie and Shanahan, 2012). As a consequence, turbulence is a local spatiotemporal generalisation of the global metastability (Hancock et al., 2024).

Specifically, the local Kuramoto order parameter, $R_\lambda(\overline{x}, t)$, is defined as the modulus of the local Kuramoto order parameter for a given brain node as a function of time (see Eq. 5 in Appendix). Hence, R_λ represents the local levels of synchronisation at a given scale, λ, as a function of space, $\overline{x}$, and time, t. The turbulence measure characterizes the *brain vortex space,* R_λ, over time. The level of amplitude turbulence, D_λ, is defined as the standard deviation across time and space of the modulus of local Kuramoto order parameter (R_λ).

Moving beyond the model-free approach, the next goal becomes to develop a model-based approach (Gollo et al., 2017). As we will see later, brain dynamics can be described through a whole-brain model of coupled oscillators (Deco and Kringelbach, 2020; Deco et al., 2017b). In particular, one of the best descriptions of brain dynamics uses the *Hopf whole-brain model* (Deco et al., 2017b), describing the behaviour of a Stuart-Landau non-linear oscillating system (Hopf, 1942). As such, it is straightforward to create a whole-brain modelling approach to turbulence.

5. Model-free turbulence in empirical fMRI data

In order to demonstrate turbulence in empirical fMRI data, the model-free turbulence framework was applied to the timeseries of the fine-grained Schaefer parcellation with 1000 regions extracted from the 1003 participants from the HCP. These timeseries were grouped according to the Euclidian distance between pairwise regions (Fig. 2**A**). To demonstrate turbulence in brain dynamics, we first measure the variability across time and space of the local order Kuramoto parameter of the timeseries (Eqs. 4, 5 and 7 in the Appendix), similar to the method developed by Kuramoto and colleagues (Kawamura et al., 2007). Importantly, for this process the BOLD fMRI time series were transformed to phase space by first filtering the signals in the range between 0.008 and 0.08 Hz (standard filter for spontaneous BOLD signals) and using the Hilbert transform to extract the evolution of the phases of the signal for each brain node over time. In other words, the BOLD signals from different spatial parts of the brain are oscillating over time and the frequency can be extracted from the corresponding power spectrum. Different brain regions have very different signals, where some are very noisy, some are like damped oscillators while others are very regular and oscillatory.

As can be seen in Fig. 2**B** (left panel) amplitude turbulence is present only in the empirical data and not in the surrogate data (which is a shuffled version maintaining the spatiotemporal characteristics of the

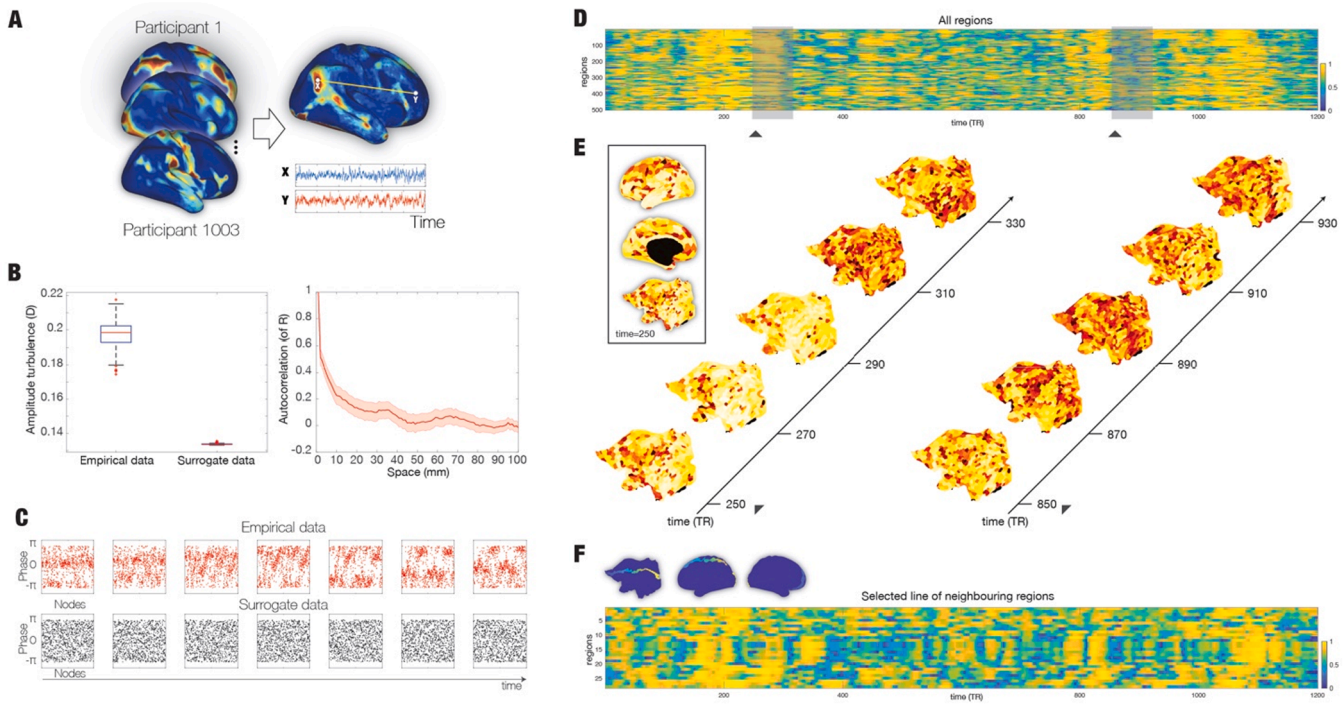

Fig. 2. Turbulence modelled with coupled oscillators. A) The timeseries of the fine-grained Schaefer parcellation with 1000 regions were extracted from state-of-the-art resting state data from a large set of 1003 healthy human participants in the Human Connectome Project (HCP) database. These were grouped according to the Euclidian distance between pairwise regions. **B)** The boxplot (left panel) shows amplitude turbulence in the empirical resting state data and not in the carefully matched surrogate data, which were significantly different ($P < 0.001$, two-sided Wilcoxon rank sum test). The right panel shows the autocorrelation of the local Kuramoto order parameter across space and time. The rapid decay demonstrates absence of regular spatiotemporal patterns in the empirical data. **C)** The figures demonstrate the presence of turbulence by plotting consecutive snapshots over time of the phases of all brain regions for both the empirical data (top) and the surrogate data (bottom). This clearly shows the absence of structure in the surrogate data and clustering resembling vortices in the empirical data. **D)** The figure visualises the change over time and space of the local Kuramoto order parameter, R, reflecting amplitude turbulence in a single participant. Amplitude turbulence can be clearly seen in the 2D plot of all 500 parcels in the left hemisphere over the 1200 timepoints. **E)** This can be appreciated from the continuous snapshots for two segments separated in time (left and right parts) rendered on a flatmap of the hemisphere (see insert with renderings of a single snapshot on the inflated and flatmapped cortex). **F)** The synchronisation of clusters over time is dependent on the neighbourhood and so to further visualise the spatiotemporal evolution of amplitude turbulence, we show a 2D plot of 26 neighbouring parcels running from the front to the back of the brain (see blue insert).

empirical data (Kantz and Schreiber, 1997)). Furthermore, the absence of regular spatiotemporal patterns in the empirical data can be seen through the autocorrelation of the local Kuramoto order parameter across spacetime (right panel), showing a rapid decay in turbulence, as predicted. Examples of turbulence is depicted through the temporally consecutive snapshots of phases of all brain regions for the empirical data (top) showing something clustering resembling vortices, which is absent in the surrogate data (bottom) (Fig. 2**C**).

Further demonstrating the turbulence found in neuroimaging data, Fig. 2**D** shows the spacetime changes in the local Kuramoto order parameter as the spatiotemporal evolution of amplitude turbulence. Specifically, we show the empirical data of a single participant in a 2D plot of all 500 parcels in the left hemisphere over the 1200 timepoints. These findings, however, do not depict the true spatiotemporal evolution of amplitude turbulence, given that this is a simplification of the 3D space through a 1D representation, and the 500 parcels are not ordered in terms of spatial neighbourhood. Rather, to appreciate the synchronisation of neighbouring clusters over time, Fig. 2**E** shows snapshots for two time-distinct segments (the left and right parts marked on the 2D plot) rendered on a flatmap of the hemisphere. In the original paper, the clear vorticity of the local synchronisation is made evident through the inclusion of time evolving videos. Furthermore, Fig. 2**F** shows an alternative representation of this by plotting only 26 neighbouring parcels, from the front to the back of the brain.

6. Whole-brain modelling of turbulence

The Hopf whole-brain model was used to model turbulence in brain dynamics as this is a system of coupled-oscillators, which can show turbulence dependent on coupling strength. Research has shown that the synchronous behaviour of brain dynamics can be modelled by coupled Stuart-Landau oscillators models (Hopf models) which can be derived from biophysical neuronal models using exact mean field models (Perl et al., 2023b). This is the reason for the successful modelling of this system with anatomically coupled Hopf oscillators (Hopf, 1942), i.e. a system of Stuart-Landau non-linear oscillators (Deco et al., 2017b). The whole-brain model used the dynamic intrinsic backbone of the anatomical brain connectivity, allowing for understanding of the mechanisms underlying turbulence. Moving to the whole-brain level, coupled together with the brain network architecture, the complex interactions between Hopf oscillators have been shown to reproduce significant features of brain dynamics observed in electrophysiology (Freyer et al., 2011; Freyer et al., 2012), MEG (Deco et al., 2017a) and fMRI (Deco et al., 2019; Kringelbach et al., 2020).

The structural connectivity matrix was constructed using the well-known *Exponential Distance Rule (EDR)* of anatomical connections as a cost-of-wiring principle. Massive tract-tracing studies have shown that the anatomical architecture of the mammalian cortex uses simple short-range wiring with an exponential drop off in strength over distance (Ercsey-Ravasz et al., 2013; Gămănuţ et al., 2018; Theodoni et al., 2020) (see fitting to empirical tractography in Fig. 3**A-D**).

The whole-brain model used Stuart-Landau oscillators with the fitted

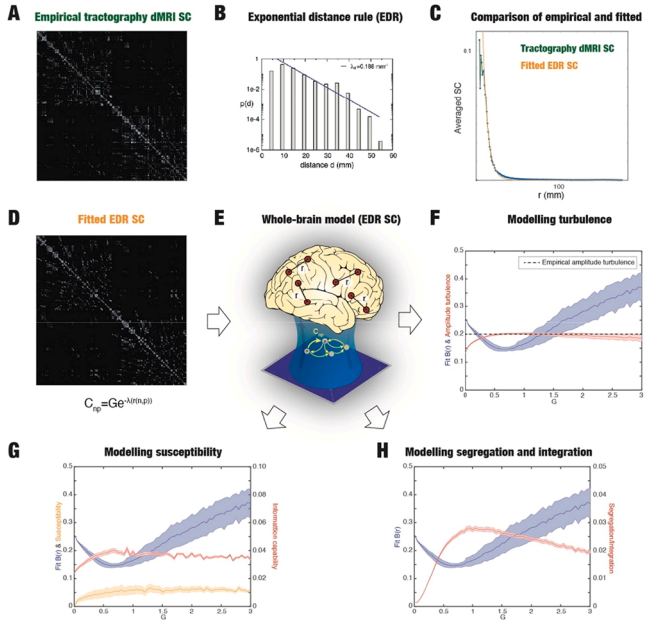

Fig. 3. Whole-brain modelling of turbulence. A) The structural connectivity (SC) matrix of the empirical data was estimated using tractography. **B)** It has been shown that the underlying brain connectivity in mammals follows the exponential decay described by the Exponential Distance Rule (Ercsey-Ravasz et al., 2013). The figure shows the histogram of interareal projection length for all labeled neurons (n = 6494,974) in a massive tract tracing study in non-human primates. The line shows the exponential fit with a decay rate 0.188 mm^{-1}. **C)** The Exponential Distance Rule is also evident in the empirical HCP dMRI tractography of the human brain, as shown by the fibre densities between the pairs of regions in the Schaefer parcellations as a function of the Euclidian distance between the nodes with green showing dMRI tractography and orange line showing the fitted Exponential Distance Rule at the optimal $\lambda = 0.18\ mm^{-1}$. The remarkable similarity can be appreciated by comparing the curves. **D)** The SC matrix shows the optimally fitted Exponential Distance Rule, which was used as the basis for the whole-brain model. **E)** The whole-brain model was based on Stuart-Landau oscillators (Deco et al., 2017b) aiming to establish the causal mechanisms underlying the emergence of turbulence. **F)** The plot shows the whole brain fit of the root squared error between the empirical and simulated B(r) in the inertial subrange as a function of the global coupling parameter G (black). The model shows amplitude turbulence (red line) in a broad range of G but maximal amplitude turbulence is found at the optimal working point fitting the data (G=0.8). The dotted line shows the amplitude turbulence estimated from the empirical data, and it is interesting that the model at the optimal working point also corresponds to this value. **G)** The maximal amplitude turbulence is likely to reflect an optimal level of information processing, which we quantify in a measure of information capability, a meaningful extension of the standard concept of susceptibility. As can be seen the maximum of information capability (red line) is found at G= 0.8 which corresponds to the optimal fitting of the whole-brain model to the empirical data (black line) and maximal amplitude turbulence. In contrast, the simple measure of susceptibility (orange line) is high but not maximal at the working point. **H)** Interestingly at the optimal point where the whole-brain model fits the empirical data (black line) and shows maximal amplitude turbulence and information capability, we also find an optimal balance between segregation/integration (red line) as a function of G.

EDR SC matrix (Deco and Kringelbach, 2020). Running this whole-brain model across coupling strengths produces a plot of the whole brain fit of the root squared error between the empirical and simulated B(r) in the inertial subrange as a function of the global coupling parameter G (black, Fig. 3**E**). The model shows amplitude turbulence (red line) in a broad range of G but maximal amplitude turbulence is found at the optimal working point fitting the data (G=0.8). The dotted line shows the amplitude turbulence estimated from the empirical data, and it is interesting that the model at the optimal working point also corresponds to this value.

Equally, the model also shows the point of maximal amplitude turbulence, reflecting the optimal level of information processing. This can be quantified in a measure of information capability, a meaningful extension of the standard concept of susceptibility. Susceptibility of the whole-brain model is the sensitivity of the brain to the processing of external stimulations. As can be seen from Eq. 8 in the Appendix, susceptibility is produced by changing the bifurcation parameter of the Hopf model to become more noisy or more oscillatory, which is producing the same effect as an external oscillatory stimulation (Escrichs et al., 2022).

We perturbed the Hopf whole-brain model at each G by randomly changing the local bifurcation parameter (a). This allowed us to estimate the sensitivity of these perturbations on the spatiotemporal dynamics by measuring the local Kuramoto order parameter. The *information capability* of the whole-brain model is a measure of how different external stimulations are encoded in the existing dynamics. The results show that the maximum of information capability (red line) is found at G= 0.8 which corresponds to the optimal fitting of the whole-brain model to the empirical data (black line) and maximal amplitude turbulence (Fig. 3**F**). In contrast, the simple measure of susceptibility (orange line) although high, is not maximal at the working point. This is highly interesting since normal susceptibility should not necessarily be maximal at the optimal working point. Maximal susceptibility typically occurs near critical transitions, but operating too close to a critical point may carry risks, such as the potential transition into a super-critical phase. Additionally, proximity to criticality can lead to critical slowing down, which might hinder computational efficiency. For optimal computation, which balances multiple factors, the system might be expected to remain at least slightly subcritical.

The model can further estimate global integration and segregation. Fig. 3**H** shows that at the optimal point where the whole-brain model fits the empirical data (black line) and is exhibiting maximal amplitude turbulence, an optimal balance between segregation and integration (red line) is observed as a function of coupling strength.

In summary, similar to the 1D ring toy model of coupled oscillators introduced by Kuramoto and colleagues (Kawamura et al., 2007), we have shown in empirical data that turbulence arises in 3D space and time from the underlying EDR brain connectivity between coupled oscillators.

7. Discovering the role of exceptional long-range connections

Moving beyond the ubiquitous EDR structure of physical systems, the brain is likely unique in terms of its complex architecture spanning multiple scales (Changeux et al., 2021). Unlike other known physical systems, where the elements communicate with nearest and close neighbouring elements (such as for example fluids or the heart), the brain uniquely possesses distant connections including a small contingent of long-range anatomical outliers. These long-range exceptions have a significant role for enhancing information processing, presumably under strong evolutionary pressure.

Uniquely, whole-brain modelling offers the possibility to test the importance of rare long-range (LR) exceptions for the brain's information processing capabilities. Two models were created using structural connectivity with rare long-range exceptions (EDR+LR) and without (EDR). These were tested on the HCP dataset of 1003 subjects. Fig. 4 shows that the inclusion of long-range exceptions confers a significant improvement in information processing as measured through turbulence, using both model-free and model-based measures.

In terms of the model-free measures, Fig. 4**C** shows significant differences in average values of FC long-range (with distances over 40 mm) for the EDR+LR model compared to the EDR model. Similarly, the boxplot in Fig. 4**D** shows a larger information cascade for the EDR+LR model compared to the EDR model. This confirms the significant role of LR exceptions in increasing the information cascade.

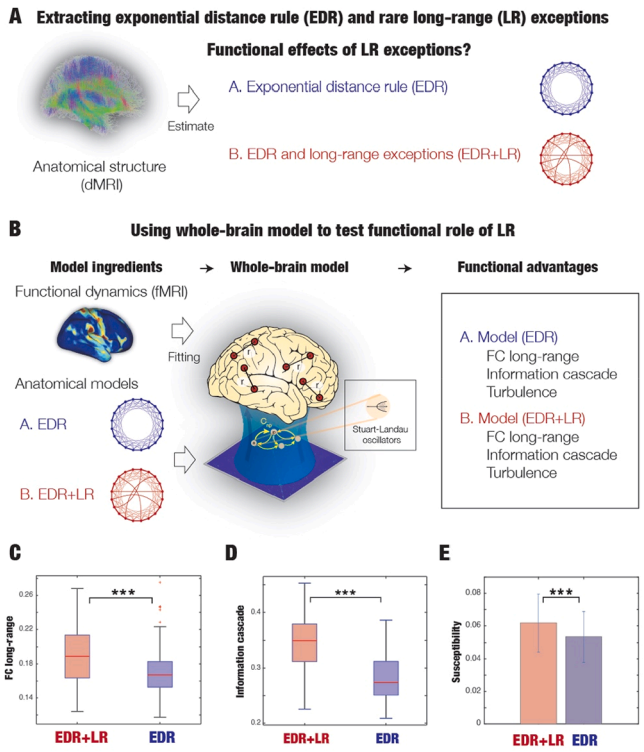

Fig. 4. Rare long-range exceptions are essential to the efficiency of turbulent information processing. Massive tract-tracing studies in primates have revealed the simple, yet powerful economy of anatomy as a cost-of-wiring principle of rare long-range exceptions on top of an exponential distance rule. Whole-brain modelling provided a unique opportunity to disentangle the functional role of these long-range exceptions by testing alternative hypotheses. **A)** First, human diffusion MRI was used to fit the exponential distance rule (EDR) and extract rare long-range exceptions on top of these (EDR+LR). The two different anatomical hypotheses are illustrated by the cartoon of two rings (EDR in blue and EDR+LR in red). **B)** Second, two different whole-brain models using these anatomical hypotheses were fitted the functional MRI data from 1003 participants. At the optimal working point, these Hopf models were able to reproduce the empirical whole-brain dynamics that emerges from the local dynamics of each brain region (described using a Stuart-Landau oscillator) coupled through the two different underlying anatomical hypotheses. **C)** The boxplot shows the mean values of the FC long-range (involving pairs with distances over 40 mm) for the two models across 100 trials. There is a significant increase for the EDR+LR model ($p < 0.001$, Wilcoxon rank sum), which shows the important role of long-range exceptions. **D)** The boxplot shows the results of investigating the role of LR exceptions in information processing by measuring the information cascade. This confirms the significant role ($p < 0.001$, Wilcoxon rank sum) for LR exceptions in increasing the information cascade (compare the EDR+LR with EDR boxplots). The information cascade is the integration of information cascade flow across scales. **E)** Using whole-brain modelling allows to measure the susceptibility (the reaction of the model to external perturbation) of the two models and again the EDR+LR model outperforms the EDR model. Overall, the findings confirm how rare long-range exceptions to the anatomical exponential distance rule are key to the efficiency of turbulent information processing.

As for the more sensitive model-based measures, Fig. 4**D** shows that in terms of susceptibility, the EDR+LR model outperforms the EDR model. The findings confirm how rare long-range exceptions to the anatomical exponential distance rule are key to the efficiency of turbulent information processing.

Beyond the fundamental properties of information processing in the brain, it is of considerable interest to note that a simplified ring architecture has been used to bolster the role of long-range exceptions (independent of the spatial location) (Deco et al., 2021b).

Overall, these results confirm the hypothesis that turbulence provides the underlying functional regime allowing for the enhanced information processing at the whole-brain level provided by the long-range connectivity.

8. Turbulence fingerprint of different brain states

Together, the model-free and model-based approaches to turbulence enable effective characterisation of different brain states. These approaches can be further refined to be more discerning by not simply taking a fixed spatial scale (as above) but by accounting for varying spatial scales, capturing the *brain vortex space*.

The concept of local metastability not only enables generalisation of vorticity in fluid dynamics but also, importantly, provides a mechanistic explanation of why such turbulent information transfer is highly efficient. More specifically, the *turbulent information cascade* can be defined by the hierarchical transfer of information across scales. This measure of *brain vortex space,* R_λ, over time, can be interpreted as the rotational vortices found in fluid dynamics, although of course the two are not identical. As such the *information cascade flow* is the predictability of a given brain vortex space at scale λ from the brain vortex space at scale $\lambda - \Delta\lambda$ (where $\Delta\lambda$ is the discretisation of scale). In other words, the measure captures information transfer across scales through local synchronisation in brain vortex space. This allows us to define the *information cascade* as the average of the *information cascade flow* across different scales. Therefore, an enhanced information cascade is a signature of enhanced information processing or enhanced information transfer across spacetime. This measure captures information transmission as mediated by local synchronisation levels at varying spatial scales. The precise mathematical definitions can be found in the published papers (Cruzat et al., 2022; Deco et al., 2023; Deco et al., 2021b; Escrichs et al., 2022).

Fig. 5 shows examples of how these model-free and model-based measures can be used to distinguish between the brain states of meditation, sleep and disorders of consciousness (Escrichs et al., 2022). In all three cases, the level of turbulence was computed for the different brain states on spatial scales from $\lambda = 0.01$ (100 mm) to $\lambda = 0.3$ (3 mm). The first panel in Fig. 5**A** shows the differences for $\lambda = 0.12$. As can be seen, the deep sleep, minimally conscious and unresponsive wakefulness states show significantly lower turbulence than healthy resting state. In contrast, at this spatial scale, meditation does not show a significant difference in turbulence compared with the resting state. The second panel of Fig. 5**A** provides a summary of all the spatial scales, which reveals significant differences at other spatial scales for meditation as well as for the other states – highlighting the informativeness of using different values of λ, covering the different spatial scales. Note especially how the evolution across spatial scales are different for different states of consciousness. Fig. 5**B** demonstrates that the model-based approach is more sensitive and shows significant differences in susceptibility and information capability for all brain states.

Finally, Fig. 5**C** shows how turbulence can provide a fingerprint of individual brain states through generation of spiderweb plots of turbulence levels in Yeo networks estimated through node-level turbulence.

A similar approach was used on other brain states, such as those elicited by psychedelics (LSD and psilocybin) (Cruzat et al., 2022) or those found in different periods of the menstrual cycle (De Filippi et al., 2021). Here again, the measurements were able to clearly distinguish between the brain states.

9. Turbulence in fast brain dynamics

This perspective has shown turbulence in whole-brain networks derived from slow haemodynamic signals measured with fMRI. However, turbulence has also been found in fast *local* hippocampal circuits (Sheremet et al., 2019), as well as fast whole-brain dynamics measured with magnetoencephalography (Deco et al., 2023). The latter provides new, deep insight suggesting turbulence could be the skeleton

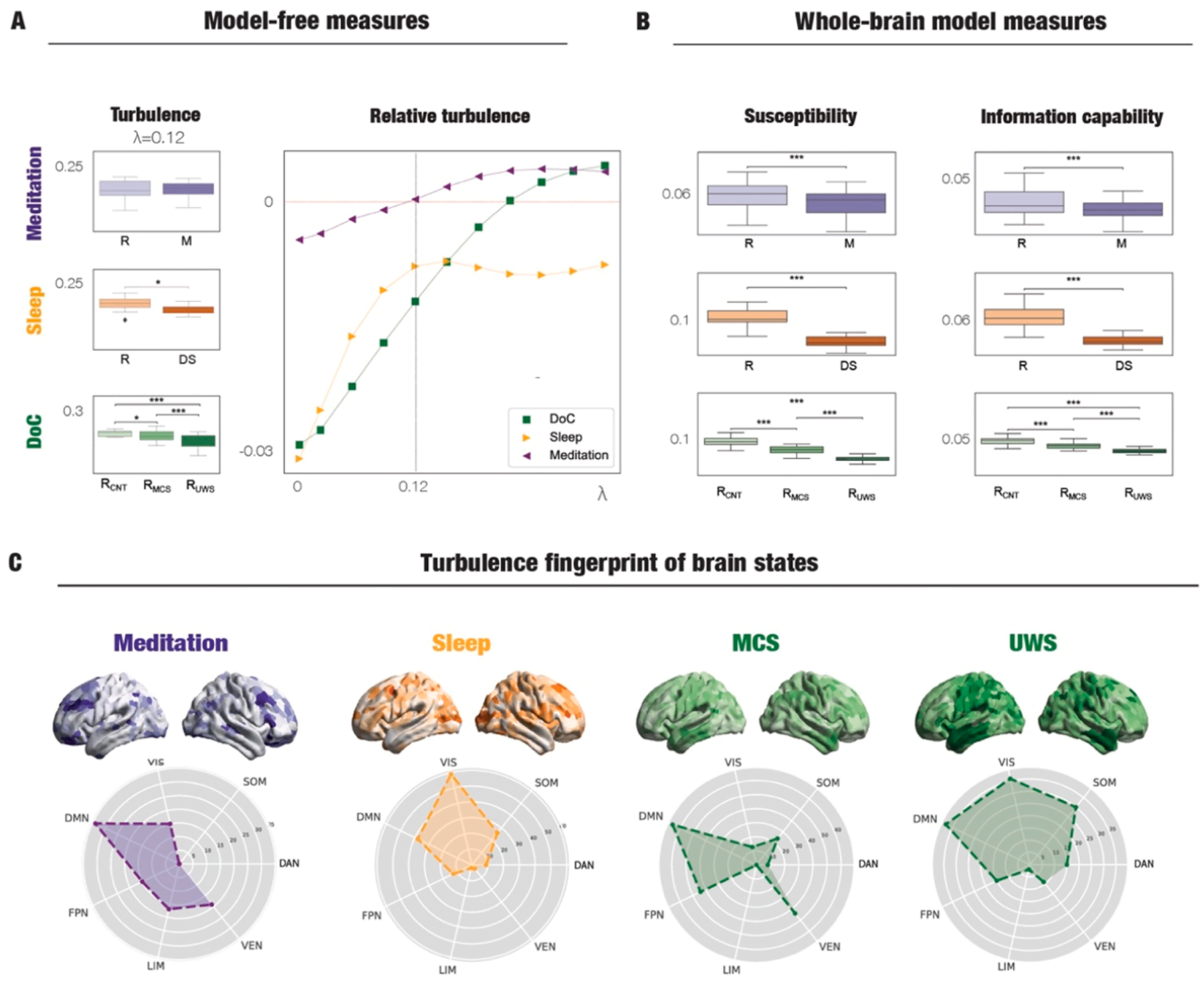

Fig. 5. ***Turbulence describes key features of different brain states.*** *The turbulence framework provides precise model-free and model-based quantification of the dynamics underlying any brain state. Here we show examples how this can be used to characterise the differences between neuroimaging data of meditation, sleep and disorders of consciousness.* ***A)*** *The level of turbulence was estimated for different brain states on spatial scales from λ= 0.01 (100 mm) to λ= 0.03 (3 mm). Here we show the differences for λ= 0.12, where the deep sleep, R_{MCS} and R_{UWS} states show significantly lower turbulence than resting state. In contrast at this spatial scale, meditation does not show a significant difference in turbulence compared with the resting state. However, as can be seen from the summary of all the spatial scales, there are significant difference at other spatial scales for meditation and the other states.* ***B)*** *As can be seen, the model-based approach is more sensitive and shows significant differences in susceptibility and information capability for all brain states.* **C)** Turbulence provides a convenient way of visualising a fingerprint of different brain states**.** The node-level turbulence can be computed as the standard deviation across time of the local Kuramoto order parameter. Here is shown brain renderings of meditation, deep sleep and disorders of consciousness (minimal conscious state, MCS and unresponsive wakefulness syndrome, UWS) as the absolute difference of the node-level of turbulence between each brain state in each dataset for scale λ = 0.12. Generating the fingerprint for each brain state as a spiderweb graph is done by picking the upper 15 % quantile of the absolute difference of the node-level turbulence between conditions, indexed the resting-state Yeo network to which they belong and estimated the number of nodes per network. Here, the spiderweb charts graphs outline the number of nodes in the higher 15 % quantile of the absolute difference for each comparison and network (VIS: visual; SOM: somatomotor; DAN: dorsal attention network; VEN: ventral network; LIM: limbic; FPN: frontoparietal network; DMN: default-mode network.).

underlying efficient spatiotemporal information transfer required for survival. The key insight as to how turbulence facilitates efficient information transfer across scales, comes from the definition of a vorticity in neural dynamics as the local level of synchronisation.

One problem with using fMRI is that it is both relatively slow with a timescale of seconds due to haemodynamic response (Kwong et al., 1992) and that it does not directly measure neural dynamics. Therefore, we used MEG, a neuroimaging modality directly measuring fast neuronal dynamics at the whole-brain level (Hansen et al., 2010). To do this, a new method was needed to overcome the problem of MEG having less accurate spatial resolution than fMRI, that is much more coarse grained brain regions. This is important since the method for demonstrating turbulence in fMRI signals requires high spatial resolution using a fine parcellation of around 1000 regions, which is difficult to obtain with MEG.

So in order to detect turbulence in fast brain dynamics, we overcame the limited number of brain regions in MEG by moving from node to edges and inventing a novel *edge metastability* measure. As the name suggests, rather than using the timeseries of *nodes*, this method relies on using the spatiotemporal variability of *edge* time series, recently introduced to capture fine-scale dynamics in fMRI recordings (Faskowitz et al., 2020; Sporns et al., 2021; Zamani Esfahlani et al., 2020). In contrast to existing methods, this novel edge metastability measure can capture turbulence with high temporal precision in a coarse-grained ring

of coupled oscillators, where the level of turbulence can be exactly analytically determined (Kawamura et al., 2007).

These methods were used to detect turbulence in spatially coarse but temporally fine MEG resting-state data from 89 participants from the HCP. Fig. 6**A** shows the pipeline of pre-processing MEG data: beamforming the sensor signals and using a DK68 parcellation (Desikan et al., 2006) to extract the signal from each coarse parcel in the five classical bands (delta 1–3 Hz, theta 3.5–7 Hz, alpha 7.5–13.5 Hz, beta 14–30.5 Hz, gamma 31–40 Hz). Please note that due to constraints in the beamforming technique, it is not possible to spatially reconstruct the signal at more than 60–90 nodes.

The results clearly show the existence of turbulence for all bands (see Fig. 6**B**) compared to circular shifted surrogate data (Deco et al., 2021c; Quiroga et al., 2002). This method generates 89 independent circular time-shifted surrogates by separately resampling the signal for each of the 89 participants. Specifically, for each timeseries of each parcel, one independent random integer c is generated within the interval [0.05 n 0.95 n] (where n is the number of time points in the timeseries signal). Then the circular time-shift is performed by moving the first c values of $X = [X_1, \ldots, X_n]$ to the end of the time series which creates the surrogate sample $X = [X_{c+1}, \ldots, X_n, X_1, \ldots, X_c]$. Such surrogates do not assume Gaussianity and have been shown to preserve the whole statistical structure of the original timeseries.

Fig. 6C shows the Edge Spacetime Predictability (ESP) measure on the MEG data (compared with surrogate data) and demonstrates significant differences for all bands.Fig. 6D **E** shows visualisations for a single participant of the edge turbulence for the five different bands for successive timepoints rendered on sideways, midline and flat map renderings of the whole brain. Fig. 6**E** displays an example of the evolution of the seven different predictions (different coloured curves, $\tau = [1..7]$) for the delta band in a specific participant as function of the Euclidean distance between parcels (x-axis). Applying edge spacetime predictability to the MEG data shows clear spacetime predictability, while applying this to the surrogate data shows no predictability. This suggests the efficiency of the turbulent regime for information transfer which is significantly better than that obtained in other regimes.

10. Conclusion

The discovery of turbulence in the human brain has provided new insights into how the brain is able to efficiently process and transmit information across time and space. The universality of turbulence has been demonstrated in many systems (L'vov, 1998) but here it provides new insight into a fundamental problem of brain function, namely how to overcome the inherent slowness of the neural responses for time-critical computation ensuring survival for the organism (Deco et al., 2023). Indeed, turbulence is a fundamental and highly useful – and almost always non-reversible – thermodynamic principle providing optimal mixing properties and allowing for the efficient transfer of energy/information over space and time (Frisch, 1995). Careful research has shown how the brain is turbulent and how the scale-free nature of turbulence provides a dynamical regime, where hierarchical

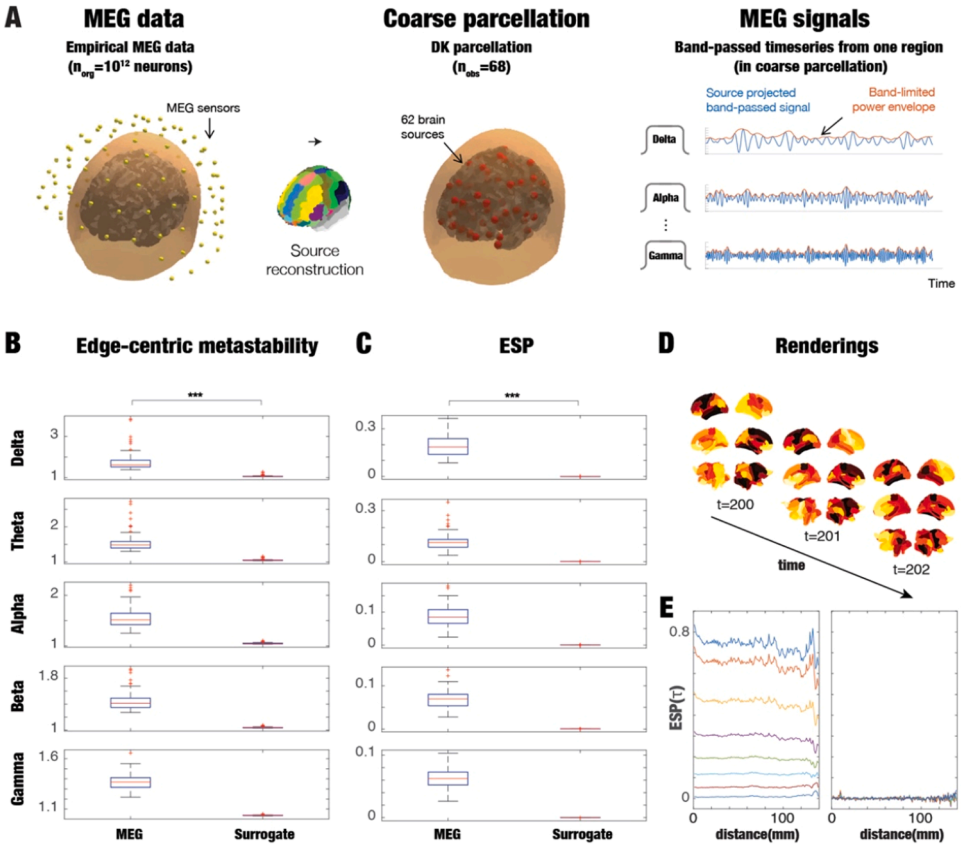

Fig. 6. Turbulence in fast MEG dynamics. A) The pipeline of pre-processing MEG data shows the sensor signals. These signals are beamformed and a coarse DK68 parcellation was used to extract the MEG signals. The third panel shows examples from each coarse parcel in the five classical bands (delta 1–3 Hz, theta 3.5–7 Hz, alpha 7.5–13.5 Hz, beta 14–30.5 Hz, gamma 31–40 Hz). **B)** The measure of edge-centric metastability shows clear turbulence for all five bands of MEG data compared to circular shifted surrogate data. **C)** Using measure of Edge Spacetime Predictability (ESP) on MEG data (compared with surrogate data), shows significant differences for all five bands, suggesting the efficiency of the turbulent regime for information transfer. **D)** Visualisations for a single participant of the edge turbulence for the delta band for three successive timepoints rendered on 3D views (sideways and midline) as well as flat map renderings of the whole brain. **E)** An example for the delta band in a specific participant of the evolution of the seven different predictions (different coloured curves, $\tau = [1..7]$) as function of the Euclidean distance between parcels (x-axis) for the empirical (left) and surrogate data (right). The error bars depict the standard error.

information cascades allow the brain to function optimally despite its relative slowness (Deco et al., 2021a; Deco and Kringelbach, 2020; Deco et al., 2021b).

In fact, turbulence has already proven to be a highly sensitive biomarker of different brain states such as sleep, coma and meditation (Escrichs et al., 2022) and psychedelics (Cruzat et al., 2022) as well as depression (Escrichs et al., 2024). In depression, the level of turbulence pre-treatment was also predictive of the treatment outcome of the pharmacological intervention (Escrichs et al., 2024).

Importantly, as shown in the work of Sanz Perl and colleagues (Perl et al., 2023a), the fact that turbulence uses higher order scaling exponents makes it an excellent framework for distinguishing between criticality as found in equilibrium systems, which are, in most cases, scale invariant – and in out-of-equilibrium systems, which, as in the paradigmatic case of turbulence, display deviations from scale invariance associated with their dissipative and forced nature.

Moving forward, at the microscopic level Maurer and colleagues have demonstrated turbulence (Sheremet et al., 2019) but the underlying microcircuitry should be further explored to see how information cascades to higher levels of organisation. This could help determine how cross-frequency coupling is a general rule, making oscillations interdependent.

At the macroscopic level, the interacting turbulent vortices express the levels of local synchronisation in the underlying brain signals, in other words a 'turbulent vortex space' a more space for describing the information processing underlying the necessary computation for behaviour (Xu et al., 2023). This vortex space offers an excellent abstraction for capturing the mechanisms underlying the orchestration of brain function over spacetime. Furthermore, this space could be used to find novel ways of controlling the turbulent vortices in disease using whole-brain modelling. One obvious prediction is that the interactions of vortices in vortex space will change in disease, and that careful modelling of these vorticity interactions will allow for better control in the brain. Another prediction is that the hierarchical orchestration of brain function at the vortex level is likely to be more informative of the underlying evolutionary principles and that this orchestration is different across species.

Overall, turbulence is ubiquitous in nature and was also recently found in the brain. Turbulence offers the tantalising prospect of understanding key mechanisms underlying the efficient spatiotemporal information transfer necessary for survival. Understanding how turbulence changes in health and disease also offers the potential for developing new strategies for controlling turbulence and thereby offering new routes to flourishing (Kringelbach et al., 2024).

Acknowledgements

G.D. is supported by Grant PID2022-136216NB-I00 funded by MICIU/AEI/10.13039/501100011033 and by "ERDF A way of making Europe", ERDF, EU, Project NEurological MEchanismS of Injury, and Sleep-like cellular dynamics (NEMESIS) (ref. 101071900) funded by the EU ERC Synergy Horizon Europe, and AGAUR research support grant (ref. 2021 SGR 00917) funded by the Department of Research and Universities of the Generalitat of Catalunya. Y.S.P. is supported by was supported by European Union's Horizon 2020 research and innovation program under the Marie Sklodowska-Curie grant 896354 and the project NEurological MEchanismS of Injury, and Sleep-like cellular dynamics (NEMESIS) (ref. 101071900) funded by the EU ERC Synergy Horizon Europe. M.L.K. is supported by the Centre for Eudaimonia and Human Flourishing (funded by the Pettit and Carlsberg Foundations) and Center for Music in the Brain (funded by the Danish National Research Foundation, DNRF117).

Appendix. : Relevant turbulence equations

In turbulence the '*structure functions*' of a variable u usually have a transversal or longitudinal fluid velocity, which can be written:

$$S(\mathrm{r}) = \left\langle (u(\overline{x}+r) - u(\overline{x}))^2 \right\rangle = 2[B(0) - B(\mathrm{r})] \tag{1}$$

In Eq. 1, the basic spatial correlations of two points separated by Euclidean distance r, given by:

$$B(r) = \langle u(\overline{x}+r)u(\overline{x}) \rangle \tag{2}$$

where the symbol $\langle\rangle$ refers to the average across the spatial location $\overline{x}$ of the nodes and time.

The extended Kolmogorov theory for higher orders (p > 2) claims that the scaling results generalize to 'structure functions' of any order

$$S_p(r) = \langle (u(\overline{x}+r) - u(\overline{x}))^p \rangle \tag{3}$$

Specifically, the local Kuramoto order parameter, $R_\lambda(\overline{x}, t)$, is defined as the modulus of the local Kuramoto order parameter for a given brain node as a function of time:

$$R_\lambda(\overline{x}, t) = \left\| \mathrm{k} \int_{-\infty}^{\infty} d\overline{x}' G_\lambda(\overline{x} - \overline{x}') e^{i\varphi(\overline{x}', t)} \right\| \tag{4}$$

where $\|\|$ is the modulus of the complex number, G_λ is the local weighting kernel $G_\lambda(\overline{x}) = e^{-\lambda|\overline{x}|}$, $\varphi(\overline{x}, t)$ are the phases of the spatiotemporal data, k is the normalisation factor $[\int_{-\infty}^{\infty} d\overline{x} G_\lambda(\overline{x} - \overline{x}')]^{-1}$, and λ defines the spatial scaling. Hence, R_λ represents the local levels of synchronisation at a given scale, λ, as function of space, $\overline{x}$, and time, t. Inspired by the rotational vortices found in fluid dynamics, the turbulence measure characterizes the *brain vortex space,* R_λ, over time.

The level of amplitude turbulence, D_λ, is defined as the standard deviation across time and space of the modulus of local Kuramoto order parameter (R_λ).

$$D_\lambda = \langle {R_\lambda}^2 \rangle_{\overline{x},t} - \langle R_\lambda \rangle_{\overline{x},t}^2 \tag{5}$$

where the brackets $\langle\rangle_{\overline{x},t}$ denote averages across time and space.

Massive tract-tracing studies have shown that the anatomical architecture of the mammalian cortex uses simple short-range wiring with an exponential drop off in strength over distance (Ercsey-Ravasz et al., 2013; Gămănuţ et al., 2018; Theodoni et al., 2020). Mathematically this can

expressed as an exponential decay function:

$$C_{np} = e^{-\lambda(r(n,p))} \tag{6}$$

where r(n, p) is the Euclidean distance between the regions n and p, and where the spatial decay $\lambda = 0.18\ mm^{-1}$ estimated from fitting the EDR rule to empirical tractography

We define the susceptibility of a whole-brain model as the sensitivity of the brain to the processing of external stimulations. We perturb the Hopf whole-brain model at each G by randomly changing the local bifurcation parameter in the range [-0.02:0]. In this case, we define the discrete version of Eq. 4 for a given brain region n as a function of time t:

$$R_\lambda(n,t)e^{i\theta_n(t)} = \sum_p \left[\frac{C_{np}}{\sum_q C_{nq}}\right] e^{i\varphi_p(t)} \tag{7}$$

where $\varphi_p(t)$ are the phases of the BOLD time series and C_{np} the anatomical exponential distance rule connectivity matrix. The BOLD fMRI time series were transformed to phase space by first filtering the signals in the range between 0.008 and 0.08 Hz and using the Hilbert transforms to extract the evolution of the phases of the signal for each brain node over time.

We estimate the sensitivity of these perturbations on the spatiotemporal dynamics by measuring the local Kuramoto order parameter, i.e. $\widetilde{R}_\lambda^{(m)}(n,t)$ for the perturbed case, and $R_\lambda^{(m)}(n,t)$ for the unperturbed case in trial m. The susceptibility is defined in the following way:

$$\chi = \left\langle \left\langle \left\langle \widetilde{R}_\lambda^{(m)}(n,t) \right\rangle_t - \left\langle R_\lambda^{(m)}(n,t) \right\rangle_t \right\rangle_{trials} \right\rangle_s \tag{8}$$

where $\langle\rangle_t$, $\langle\rangle_{trials}$ and $\langle\rangle_s$ are the mean averages across time, trials and space, respectively.

Moving beyond susceptibility, we define the *information capability* of the whole-brain model as a measure to capture how different external stimulations are encoded in the dynamics. Specifically, we perturb the model as above, but here the information capability I is defined as the standard deviation across trials of the difference between the perturbed and unperturbed mean of the modulus of the local order parameter across time, averaged over all brain nodes n, i.e.:

$$I = \left\langle \left\langle \left(\left\langle \widetilde{R}_\lambda^{(m)}(n,t) \right\rangle_t - \left\langle R_\lambda^{(m)}(n,t) \right\rangle_t \right)^2 \right\rangle_{trials} - \left\langle \left(\left\langle \widetilde{R}_\lambda^{(m)}(n,t) \right\rangle_t - \left\langle R_\lambda^{(m)}(n,t) \right\rangle_t \right) \right\rangle_{trials}^2 \right\rangle_s \tag{9}$$

where the averages ($\langle\rangle_t$, $\langle\rangle_{trails}$ and $\langle\rangle_s$) are defined as above.

Here, integration is defined as the mean value of all functional correlation pairs i and j, i.e.

$$Y = \frac{1}{k}\sum_{i,j>i} F_{ij} = \langle u_i u_j \rangle_t \tag{10}$$

where k is the number of upper triangular elements in the functional connectivity matrix F, whose elements are defined as the temporal average of the z-scored functional signals u between regions i and j.

As a complement of the integration, we used the modularity measure (Rubinov and Sporns, 2011) as a measure of segregation. Modularity is defined as a measure of the goodness with which a network is optimally partitioned into functional subgroups, i.e. a complete subdivision of the network into non-overlapping modules, and supported by densely connected network communities. We consider the modularity of our FC matrix. Our measure of modularity is given by,

$$S = \frac{1}{v^+}\sum_{ij}(w_{ij}^+ - e_{ij}^+)\delta_{M_i M_j} \tag{11}$$

Where the total weight, $v^+ = \sum_{ij} w_{ij}^+$ is the sum of all positive or negative connection weights (counted twice for each connection), being $w_{ij}^+ \in (0,1]$ the weighted connection between regions i and j. The chance-expected within-module connection weights $e_{ij}^+ = \frac{s_i^+ s_j^+}{v^+}$, where the strength of node i, $s_i^+ = \sum_{ij} w_{ij}^+$, is the sum of positive or negative connection weights of i. The $\delta_{M_i M_j} = 1$ when i and j are in the same module and $\delta_{M_i M_j} = 0$, otherwise (Newman, 2006). For a complete description see (Sporns, 2010).

Specifically, the spatial information transfer shows how the information travels across space at a specific scale, λ. This measure is defined as the slope of a linear fitting in log-log scale of the time correlation between the local Kuramoto order parameter of two brain areas, at the same scale as a function of its Euclidean distance (r) within the inertial subrange (the limited range where turbulence energy is transferred from larger to smaller scales without loss). We used the linear fit only to quantify the level of decay of the correlation of the local level of synchronisation with distance. Please note that we compute the linear fit in a limited log-log space and, as such, we do not have a distribution, and thus not trying to fit a power law.

$$\log(corr_t(R_\lambda(\bar{x}), R_\lambda(\bar{x}+r))) = A_\lambda * \log(r) + B_\lambda \tag{12}$$

where $corr_t$ is the pairwise correlation across time, A_λ and B_λ are the fitting parameters for each scale (λ), where r is the spatial distance in the brain. The negative slope (A_λ) stands for the transfer in the spatial direction r of the information in terms of time correlation of the local level of synchronization. In this regard, when the slope is steeper, the information travels across shorter distances; while a flatter slope indicates that the information is transferred across longer distances. Thus, the negative slope stands for the spatial information transfer. Note that the parameter A only depends on λ. It does not depend on t as the correlation is over time, neither on the brain areas, as the pairwise correlations are organized as a function

of the Euclidean distances.

Complementarily, the information cascade flow characterizes the stream of information between a given scale (λ) and a subsequent lower scale ($\lambda - \Delta\lambda$, where $\Delta\lambda$ is a scale step) in consecutive time steps (t and $t + \Delta t$). In this way, the information cascade flow covers the information transfer across scales computed as the time correlation between the local Kuramoto order parameter in two consecutive scales and times:

$$\mathscr{F}(\lambda) = \langle corr_t(R_\lambda(\bar{x}, t + \Delta t), R_{\lambda-\Delta\lambda}(\bar{x}, t)) \rangle_{\bar{x}} \tag{13}$$

where the brackets $\langle\rangle_{\bar{x}}$ denote averages across time and space, and $corr_t$ refers to the pairwise time correlations. Finally, the *information cascade*, *IC*, is defined by averaging the information transfer across scales λ, capturing the entire information processing behaviour across scales, which is simply the average of $\mathscr{F}(\lambda)$ across different scales (λ):

$$IC = \langle \mathscr{F}(\lambda) \rangle_\lambda \tag{14}$$

where the symbol $\langle\rangle_\lambda$ refers to the average across λ.

Mathematically, edge metastability was applied to MEG data (see Fig. 6**A**), consisting of band-passed time series. We therefore used the standard definition of edge-centric used in fMRI (Faskowitz et al., 2020; Sporns et al., 2021; Zamani Esfahlani et al., 2020):

$$E_{i,j}(t) = Z_i(t)Z_j(t) \tag{15}$$

where Z is the z-scored Hilbert envelope of the filtered MEG signals.

Extending this for measuring information transfer, we introduced the concept of *Edge Spacetime Predictability (ESP)* as the information transfer correlation across space and time by computing the predictability of the edge measure over space and time. ESP is defined as the mean value over all pairs of the mean value of the shifted correlations across time shift $\tau = [1..7]$. Thus, for each pair i, j ESP is the shifted correlation for a given τ defined as

$$ESP_{i,j}(\tau) = \frac{\sum_t \widetilde{E}_{i,j}(t-\tau)\widetilde{E}_{i,j}(t)}{\sqrt{\widetilde{E}_{i,j}(t-\tau)^2}\sqrt{\widetilde{E}_{i,j}(t)^2}} \tag{16}$$

where $\widetilde{E}_{i,j}$ is the de-meaned version of $E_{i,j}$.

References

Baars, B.J., 1989. A Cognitive Theory of Consciousness. Cambridge University Press, Cambridge, MA.

Bewley, G.P., Lathrop, D.P., Sreenivasan, K.R., 2006. Superfluid helium: visualization of quantized vortices. Nature 441, 588.

Bouchaud, J.P., Mézard, M., Parisi, G., 1995. Scaling and intermittency in Burgers turbulence. Phys. Rev. E 52, 3656–3674.

Cabral, J., Luckhoo, H., Woolrich, M., Joensson, M., Mohseni, H., Baker, A., Kringelbach, M.L., Deco, G., 2014. Exploring mechanisms of spontaneous functional connectivity in MEG: How delayed network interactions lead to structured amplitude envelopes of band-pass filtered oscillations. Neuroimage 90, 423–435.

Changeux, J.P., Goulas, A., Hilgetag, C.C., 2021. A connectomic hypothesis for the hominization of the brain. Cereb. Cortex 31, 2425–2449.

Christoph, J., Chebbok, M., Richter, C., Schroder-Schetelig, J., Bittihn, P., Stein, S., Uzelac, I., Fenton, F.H., Hasenfuss, G., Gilmour Jr., R.F., Luther, S., 2018. Electromechanical vortex filaments during cardiac fibrillation. Nature 555, 667–672.

Cocchi, L., Gollo, L.L., Zalesky, A., Breakspear, M., 2017. Criticality in the brain: A synthesis of neurobiology, models and cognition. Prog. Neurobiol. 158, 132–152.

Cotterill, R.M.J., 2002. Biophysics. An introduction. Wiley, New York.

Cross, M.C., Hohenberg, P.C., 1993. Pattern formation outside of equilibrium. Rev. Mod. Phys. 65, 851–1112.

Cruzat, J., Perl, Y.S., Escrichs, A., Vohryzek, J., Timmermann, C., Roseman, L., Luppi, A. I., Ibañez, A., Nutt, D., Carhart-Harris, R., Tagliazucchi, E., Deco, G., Kringelbach, M. L., 2022. Effects of classic psychedelic drugs on turbulent signatures in brain dynamics. Netw. Neurosci. 6, 1104–1124.

De Filippi, E., Uribe, C., Avila-Varela, D.S., Martinez-Molina, N., Gashaj, V., Pritschet, L., Santander, T., Jacobs, E.G., Kringelbach, M.L., Sanz Perl, Y., Deco, G., Escrichs, A., 2021. The Menstrual Cycle Modulates Whole-Brain Turbulent Dynamics. Front Neurosci. 15, 753820.

Deco, G., Cabral, J., Woolrich, M., Stevner, A.B.A., Van Hartevelt, T., Kringelbach, M.L., 2017a. Single or multi-frequency generators in on-going MEG data: a mechanistic whole-brain model of empirical MEG data. Neuroimage 152, 538–550.

Deco, G., Cruzat, J., Cabral, J., Tagliazucchi, E., Laufs, H., Logothetis, N.K., Kringelbach, M.L., 2019. Awakening: predicting external stimulation forcing transitions between different brain states. PNAS 116, 18088–18097.

Deco, G., Kemp, M., Kringelbach, M.L., 2021a. Leonardo da Vinci and the search for order in neuroscience. Curr. Biol. 31, R704–R709.

Deco, G., Kringelbach, M.L., 2020. Turbulent-like dynamics in the human brain. Cell Rep. 33, 108471.

Deco, G., Kringelbach, M.L., Jirsa, V., Ritter, P., 2017b. The dynamics of resting fluctuations in the brain: metastability and its dynamical core [bioRxiv 065284]. Sci. Rep. 7, 3095.

Deco, G., Leibana Garcia, S., Sanz Perl, Y., Tagliazucchi, E., Kringelbach, M.L., 2023. The effect of turbulence in brain dynamics information transfer measured with magnetoencephalography. Commun. Phys. 6, 74.

Deco, G., Sanz Perl, Y., Vuust, P., Tagliazucchi, E., Kennedy, H., Kringelbach, M.L., 2021b. Rare long-range cortical connections enhance human information processing. Curr. Biol. 31, 1–13.

Deco, G., Vidaurre, D., Kringelbach, M.L., 2021c. Revisiting the Global Workspace orchestrating the hierarchical organisation of the human brain. Nat. Hum. Behav. 5, 497–511.

Dehaene, S., Kerszberg, M., Changeux, J.P., 1998. A neuronal model of a global workspace in effortful cognitive tasks. Proc. Natl. Acad. Sci. U. S. A. 95, 14529–14534.

Desikan, R.S., Se, F., Fischl, B., Quinn, B.T., Dickerson, B.C., Blacker, D., Buckner, R.L., Dale, A.M., Maguire, R.P., Hyman, B.T., Albert, M.S., Killiany, R.J., 2006. An automated labeling system for subdividing the human cerebral cortex on MRI scans into gyral based regions of interest. NeuroImage 31, 968–980.

Ercsey-Ravasz, M., Markov, N.T., Lamy, C., Van Essen, D.C., Knoblauch, K., Toroczkai, Z., Kennedy, H., 2013. A predictive network model of cerebral cortical connectivity based on a distance rule. Neuron 80, 184–197.

Escrichs, A., Sanz Perl, Y., Fisher, P.M., Martinez-Molina, N., E, G.G., Frokjaer, V.G., Kringelbach, M.L., Knudsen, G.M., Deco, G., 2024. Whole-brain turbulent dynamics predict responsiveness to pharmacological treatment in major depressive disorder. Mol. Psychiatry.

Escrichs, A., Sanz Perl, Y., Uribe, C., Camara, E., Turker, B., Pyatigorskaya, N., Lopez-Gonzalez, A., Pallavicini, C., Panda, R., Annen, J., Gosseries, O., Laureys, S., Naccache, L., Sitt, J.D., Laufs, H., Tagliazucchi, E., Kringelbach, M.L., Deco, G., 2022. Unifying turbulent dynamics framework distinguishes different brain states. Commun. Biol. 5, 638.

Faskowitz, J., Esfahlani, F.Z., Jo, Y., Sporns, O., Betzel, R.F., 2020. Edge-centric functional network representations of human cerebral cortex reveal overlapping system-level architecture. Nat. Neurosci. 23, 1644–1654.

Fregnac, Y., 2017. Big data and the industrialization of neuroscience: A safe roadmap for understanding the brain? Science 358, 470–477.

Freyer, F., Roberts, J.A., Becker, R., Robinson, P.A., Ritter, P., Breakspear, M., 2011. Biophysical mechanisms of multistability in resting-state cortical rhythms. J. Neurosci. 31, 6353–6361.

Freyer, F., Roberts, J.A., Ritter, P., Breakspear, M., 2012. A canonical model of multistability and scale-invariance in biological systems. PLoS Comput. Biol. 8, e1002634.

Frisch, U., 1995. Turbulence: The Legacy of A. N. Kolmogorov. Cambridge University Press, Cambridge.

Friston, K., 2010. The free-energy principle: a unified brain theory? Nat. Rev. Neurosci. 11, 127–138.

Gămănuț, R., Kennedy, H., Toroczkai, Z., Ercsey-Ravasz, M., Van Essen, D.C., Knoblauch, K., Burkhalter, A., 2018. The mouse cortical connectome, characterized

by an ultra-dense cortical graph, maintains specificity by distinct connectivity profiles. Neuron 97, 698–715.
Gollo, L.L., Roberts, J.A., Cocchi, L., 2017. Mapping how local perturbations influence systems-level brain dynamics. NeuroImage 160, 97–112.
Hancock, F., Rosas, F.E., Zhang, M., Mediano, P.A.M., Luppi, A., Cabral, J., Deco, G., Kringelbach, M., Breakspear, M., Kelso, J.A.S., Turkheimer, F.E., 2024. Metastability demystified — the foundational past, the pragmatic present and the promising future. Nature Reviews Neuroscience. https://doi.org/10.1038/s41583-41024-00883-41581.
Hansen, P.C., Kringelbach, M.L., Salmelin, R., 2010. MEG. An introduction to methods. Oxford University Press, Oxford.
Hodgkin, A.L., Huxley, A.F., 1952a. A quantitative description of membrane current and its application to conduction and excitation in nerve. J. Physiol. 117, 500–544.
Hodgkin, A.L., Huxley, A.F., 1952b. A quantitative description of membrane current and its application to conduction and excitation in nerve. J. Physiol. (Lond. 117, 500–544.
Hopf, E., 1942. Abzweigung einer periodischen Lösung von einer stationären Lösung eines Differentialsystems. Ber. Verh. Sächs. Akad. Wiss. Leipz., Math. -Nat. Kl. 94, 3–22.
Itoh, K., Konoike, N., Nejime, M., Iwaoki, H., Igarashi, H., Hirata, S., Nakamura, K., 2022. Cerebral cortical processing time is elongated in human brain evolution. Sci. Rep. 12, 1103.
Kantz, H., Schreiber, T., 1997. Nonlinear time series analysis. Cambridge University Press, Cambridge.
Kawamura, Y., Nakao, H., Kuramoto, Y., 2007. Noise-induced turbulence in nonlocally coupled oscillators. Phys. Rev. E, Stat., Nonlinear, soft Matter Phys. 75, 036209.
Kelso, J.A.S., 1995. Dynamic Patterns: The Self-Organization of Brain and Behavior. MIT Press, Cambridge, MA.
Kelty-Stephen, D.G., Palatinus, K., Saltzman, E., Dixon, J.A., 2013. A tutorial on multifractality, cascades, and interactivity for empirical time series in ecological science. Ecol. Psychol. 25, 1–62.
Kitzbichler, M.G., Smith, M.L., Christensen, S.R., Bullmore, E., 2009. Broadband criticality of human brain network synchronization. PLoS Comput. Biol. 5, e1000314.
Kolmogorov, A.N., 1941a. Dissipation of energy in locally isotropic turbulence. Proc. USSR Acad. Sci. (Russ.) 32, 16–18.
Kolmogorov, A.N., 1941b. The local structure of turbulence in incompressible viscous fluid for very large Reynolds numbers. Proc. USSR Acad. Sci. (Atmos. Ocean. Phys.) 30, 299–303.
Kringelbach, M.L., Cruzat, J., Cabral, J., Knudsen, G.M., Carhart-Harris, R.L., Whybrow, P.C., Logothetis, N.K. and Deco, G. (2020) Dynamic Coupling of Whole-Brain Neuronal and Neurotransmitter Systems. PNAS, in press.
Kringelbach, M.L., Deco, G., 2020. Brain states and transitions: insights from computational neuroscience. Cell Rep. 32, 108128.
Kringelbach, M.L., Sanz Perl, Y., Deco, G., 2024. The Thermodynamics of Mind. Trends Cogn. Sci.
Kringelbach, M.L., Vuust, P., Deco, G., 2024. Building a science of human pleasure, meaning making, and flourishing. Neuron 112, 1392–1396.
Kuramoto, Y., 1984. Chemical Oscillations,Waves, and Turbulence. Springer-Verlag, Berlin.
Kwong, K.K., Belliveau, J.W., Chesler, D.A., Goldberg, I.E., Weisskoff, R.M., Poncelet, B. P., Kennedy, D.N., Hoppel, B.E., Cohen, M.S., Turner, R., Cheng, H.M., Brady, T.J., Rosen, B.R., 1992. Dynamic magnetic resonance imaging of human brain activity during primary sensory stimulation. Proc. Natl. Acad. Sci. U. S. A. 89, 5675–5679.
L'vov, V.S., 1998. Universality of turbulence. Nature 396, 519–521.
Laurenza, D., Kemp, M. (Eds.), 2019. Codex Leicester: Leonardo da Vinci. A New Edition of the Codex Leicester of Leonardo da Vinci, 4 vols. Oxford University Press, Oxford.
Likens, A.D., Fine, J.M., Amazeen, E.L., Amazeen, P.G., 2015. Experimental control of scaling behavior: what is not fractal? Exp. brain Res. 233, 2813–2821.
Navier, C.L.M.H., 1823. Mémoire sur les lois du mouvement des fluides. M. éM. Acad. Roy. Sci. 6, 389–440.
Newman, M.E., 2006. Modularity and community structure in networks. Proc. Natl. Acad. Sci. U. S. A. 103, 8577–8582.
Northoff, G., 2013. What the brain's intrinsic activity can tell us about consciousness? A tri-dimensional view. Neurosci. Biobehav. Rev. 37, 726–738.
Northoff, G., 2024. From brain dynamics to the mind. Spatiotemporal Neuroscience. Elsevier, New York.
Northoff, G., Huang, Z., 2017. How do the brain's time and space mediate consciousness and its different dimensions? Temporo-spatial theory of consciousness (TTC). Neurosci. Biobehav. Rev. 80, 630–645.
Oono, Y., Yeung, C., 1987. A cell dynamical system model of chemical turbulence. J. Stat. Phys. 48, 593–644.
Perl, Y.S., Mininni, P., Tagliazucchi, E., Kringelbach, M.L., Deco, G., 2023a. Scaling of whole-brain dynamics reproduced by high-order moments of turbulence indicators. Phys. Rev. Res. 5, 033183.
Perl, Y.S., Zamora-Lopez, G., Montbrió, E., Monge-Asensio, M., Vohryzek, J., Fittipaldi, S., Campo, C.G., Moguilner, S., Ibañez, A., Tagliazucchi, E., Yeo, B.T.T., Kringelbach, M.L., Deco, G., 2023b. The impact of regional heterogeneity in whole-brain dynamics in the presence of oscillations. Netw. Neurosci. 7, 632–660.
Quiroga, R.Q., Kraskov, A., Kreuz, T., Grassberger, P., 2002. Performance of different synchronization measures in real data: a case study on electroencephalographic signals. Phys. Rev. E 65, 041903.
Richardson, L.F., 1922. Weather prediction by numerical process. Cambridge University Press, Cambridge.
Rubinov, M., Sporns, O., 2011. Weight-conserving characterization of complex functional brain networks. Neuroimage 56, 2068–2079.
Shanahan, M., 2010. Metastable chimera states in community-structured oscillator networks. Chaos 20, 013108.
Sheremet, A., Qin, Y., Kennedy, J.P., Zhou, Y., Maurer, A.P., 2019. Wave turbulence and energy cascade in the hippocampus. Front. Syst. Neurosci. 12, 62.
Sporns, O., 2010. Networks of the Brain. The MIT Press.
Sporns, O., Faskowitz, J., Teixeira, A.S., Cutts, S.A., Betzel, R.F., 2021. Dynamic expression of brain functional systems disclosed by fine-scale analysis of edge time series. Netw. Neurosci. 5, 405–433.
Stokes, G.G., 1843. On some cases of fluid motion. Trans. Camb. Philos. Soc. 8, 105.
Theodoni, P., Majka, P., Reser, D.H., Wójcik, D.K., Rosa, M.G.P. and Wang, X.-J. (2020) Structural attributes and principles of the neocortical connectome in the marmoset monkey. bioRxiv, 2020.2002.2028.969824.
Tognoli, E., Kelso, J.A., 2014. The metastable brain. Neuron 81, 35–48.
Tononi, G., Sporns, O., Edelman, G.M., 1994. A measure for brain complexity: relating functional segregation and integration in the nervous system. Proc. Natl. Acad. Sci. U. S. A. 91, 5033–5037.
Wildie, M., Shanahan, M., 2012. Metastability and chimera states in modular delay and pulse-coupled oscillator networks. Chaos 22, 043131.
Xu, Y., Long, X., Feng, J., Gong, P., 2023. Interacting spiral wave patterns underlie complex brain dynamics and are related to cognitive processing. Nat. Hum. Behav. 7, 1196–1215.
Yao, H., Yeung, P.K., Zaki, T.A., Meneveau, C., 2024. Forward and Inverse Energy Cascade in Fluid Turbulence Adhere to Kolmogorov's Refined Similarity Hypothesis. Phys. Rev. Lett. 132, 164001.
Zamani Esfahlani, F., Jo, Y., Faskowitz, J., Byrge, L., Kennedy, D.P., Sporns, O., Betzel, R. F., 2020. High-amplitude cofluctuations in cortical activity drive functional connectivity. Proc. Natl. Acad. Sci. U. S. A. 117, 28393–28401.

Glossary

Chaos: Dynamical behaviour arising in a time-invariant nonlinear system, characterised by sustained aperiodic (nonrepeating) oscillations, where small changes in present values of the system can lead to extreme sensitivity of future states.

Criticality: Dynamical systems at the brink of a bifurcation display certain characteristic dynamic features, of which most are related to enhanced fluctuations. Within statistical mechanics, the term criticality refers to the behaviour of a system near a critical point, undergoing a phase transition (such as when transitioning from liquid to gas). At this critical point, the system exhibits unique properties including long-range correlations, scale invariance and diverging quantities such as susceptibility and correlation length.

Entropy: Measure of the uncertainty or disorder associated with a random system or process. This quantifies how spread out or unpredictable the possible outcomes of the system are, based on the probabilities of different states. Entropy also reflects the amount of information needed to describe the state of the system. High entropy means that the outcomes are more spread out, and therefore, more uncertain or less predictable. Conversely, low entropy indicates that the system is more predictable, with fewer possible states having high probabilities.

Entropy production: Measure of irreversibility expressed by the Kullback-Leibler divergence between the forward and reversed backward transition probabilities in a given state space.

Generative mechanisms: The fundamental rules driving the temporal evolution of a system, where the underlying mechanisms can be derived by building a model of the system and investigating the causal influence of manipulating the model elements (also see 'whole-brain model').

Hierarchy: Stratified organisation of the different hierarchical levels of a system such as the brain. Hierarchy can be measured with a variety of mathematical tools; each providing a unique lens to understand the hierarchical flow of information in brain dynamics.

Information transfer: Quantification of information flow propagating through a system at a particular scale, which captures the directional flow and influence of information between different regions or elements.

Information cascade flow: Quantification of the directed information transfer between adjacent scales, providing an estimation of how information propagates from a higher scale to a subsequent lower scale over consecutive time steps. This concept emphasises the hierarchical flow of information, capturing how large-scale patterns or global structures influence smaller, localised dynamics.

Information cascade: Quantification of entire process of information transfer across multiple scales, encompassing both the flow of information within and between hierarchical levels. The information cascade is the average of the information cascade flow across scales.

Irreversibility: Property of a dynamical system whereby certain transitions or dynamics cannot be reversed in time. It reflects the asymmetry of time, often arising from the dissipation of energy, increase in entropy, or loss of information. In complex systems such as the brain, irreversibility is associated with the directionality of processes, such as the progression of brain states, and is essential for understanding complex phenomena like brain states and cognition within these states. Through imposing a temporal order on the sequence of states, irreversibility enhances the hierarchical complexity of the entropic dynamics of the brain. A quantification of irreversibility is entropy production which is closely related to the 'arrow of time'.

Kolmogorov scaling: A set of scaling laws describing the statistical properties of fully developed turbulence in incompressible fluids. It is based on the idea that in the inertial subrange of turbulence—where energy cascades from large to small scales without loss—turbulent dynamics are universal and determined solely by the rate of energy dissipation and the scale of the eddies. In neuroscience, it is usually reflected in the power law observed in the functional connectivity between two regions as a

function their distances.

Metastability: A state in which the brain exhibits a balance between stability and flexibility, allowing it to flexibly switch between different activity patterns, which is a measure of synchronisation (whether local or global). It can be interpreted as a quantification of the available dynamical repertoire.

Non-equilibrium thermodynamics: Important branch of thermodynamics that deals with systems that are not in a state of thermodynamic equilibrium. Unlike equilibrium thermodynamics, which describes systems where macroscopic properties (such as for example temperature and pressure) are uniform and constant over time, non-equilibrium thermodynamics studies systems where these properties are spatially and temporally varying. A fundamental feature of non-equilibrium system is its temporal irreversibility, that is the emergence of an 'arrow of time'.

Order parameter: A single variable that captures the collective or macro behaviour of a system composed of microscopic elements. In neuroscience, it conveys the synchronisation level of brain processes, offering a macroscopic view of the emergent dynamics.

Oscillator: Dynamical systems exhibiting periodic behaviour over time, characterised by the regular evolution of its state variables (such as phase and amplitude) around an equilibrium point. In neuroscience, the standard model of a perfect oscillator is the Kuramoto oscillator and a more general used oscillator is the Stuart-Landau oscillator which is defined by the normal form of a Hopf bifurcation.

Power law and scale-free dynamics: The power law indicates a special mathematical relationship between two quantities in which one quantity varies as a power of the other. The power law distribution arises when extreme events occur with low probability, such as how most people in a social network only have a couple of hundred contacts, while some influencers may have millions. The power law often indicates that a system such as the brain could be scale free and operate in a critical state of self-organised criticality, which makes the system highly robust to random failures, but vulnerable to attacks.

Turbulence: This concept was first described for fluid dynamics reaching back to Leonardo da Vinci but subsequent research has been able to show turbulence in highly variable and dynamic patterns of system exhibiting local synchronisations, characterised by significant fluctuations across space and time. This variability can be quantified using the local Kuramoto parameter, which measures the degree of local synchronisation at any given point. Conceptually, turbulence can be viewed as a spatiotemporal extension of metastability, capturing the complex interplay between order and disorder in the system. This phenomenon is particularly relevant in neural systems, where turbulence can be modelled using coupled oscillators and provide insights into the complex, non-equilibrium behaviour underlying brain function and cognition.

Vorticity: Defined in fluid dynamics as a measure of the local rotation of motion of a fluid around a specific point, which mathematically corresponds to the curl of the velocity field in the fluid. Here, the definition is extended to characterise the level of local synchronisation around a specific spatial region in the brain using the concept of the local Kuramoto order parameter.

Wave number: Measure of the spatial frequency of a wave, representing the number of wavelengths per unit distance.

Whole-brain model: Powerful tool for modelling brain dynamics from whole-brain neuroimaging techniques, such as fMRI or magnetoencephalography. In its simplest form, the whole-brain model is constructed using the anatomical connectivity of a reduced set of typically hundreds of anatomically defined brain regions. Each anatomically linked region contains a model of the local dynamics, and the model is fitted to the neuroimaging time series by simply scaling the global connectivity. The elements of such an *in silico* model of brain dynamics can then be exhaustively probed, and the underlying causal mechanisms revealed.